Proc. Indian Acad. Sci. (Chem. Sci.), Vol. 107, No. 3, June 1995, pp. 233–244.
© Printed in India.

Resonance Raman intensity analysis of polyatomic molecules

N BISWAS[1], S UMAPATHY[1]*, C KALYANARAMAN[2] and N SATHYAMURTHY[2]*

[1]Department of Inorganic and Physical Chemistry, Indian Institute of Science, Bangalore 560 012, India
[2]Department of Chemistry, Indian Institute of Technology, Kanpur 208 016, India

MS received 25 May 1995

Abstract. A time-dependent quantum mechanical (TDQM) method of wavepacket propagation in computing resonance Raman intensities for polyatomic systems, has been developed and demonstrated by applying it to *cis*-stilbene and *trans*-azobenzene. In the case of the former, Raman excitation profiles (REPs) for the various vibrational modes have also been computed. It is observed that the calculated absorption spectrum and the REPs compare very well with the experimental results. A comparison of these results with those of the often used semiclassical approach reveals that the TDQM method can be used to study polyatomic systems with as much ease as the semiclassical wavepacket method.

Keywords. Raman intensities; wavepacket theory; Raman excitation profiles; stilbene; azobenzene.

1. Introduction

Understanding the spectral and dynamical features of polyatomic molecules has been a challenging problem to both theoreticians and experimentalists. On the one hand, most real-life problems that require the attention of experimental spectroscopists, involve polyatomic systems with a large number of degrees of freedom, and on the other, interpreting the spectroscopic data quantitatively from a theoretical point of view has been a daunting task because of the formidable difficulties in dealing with a high density of states. Therefore, one is invariably forced to look at alternative strategies to learn about the dynamics of polyatomic molecules from the experimental data. One such method, time dependent wavepacket dynamics, can be used to interpret the observed resonance Raman intensities, and is discussed here.

It is known that under resonance excitation, the observed Raman intensities contain information related to the displacement of the vibrational mode in the first excited state and therefore, to the dynamics associated with it. Resonance Raman intensity analysis by the wavepacket propagation technique was first developed semiclassically (Lee and Heller 1979; Heller *et al* 1982; Tannor and Heller 1982), using the concept of localized wavepackets. Its validity even when the wavepacket is not localized has been established by Ramakrishna and Coalson (1988). Polyatomic molecules like *cis*-stilbene (Myers and Mathies 1984), bacteriorhodopsin (Myers *et al* 1983), isoprene and hexatriene (Myers *et al* 1982) have been studied using Heller's approach.

*For correspondence

In the time-dependent picture, the initial wavepacket $|i\rangle$, corresponding to the ground electronic and vibrational state, is transferred by a photon to the electronically excited state. The transposed wavepacket starts moving on the excited state surface under the influence of the excited state Hamiltonian (H_{ex}). This wavepacket $|i(t)\rangle$ moves away from the Franck–Condon region in time t. The moving wavepacket can then be overlapped with various vibrational levels $|i\rangle$ or $|f\rangle$ of the ground electronic state (where $|f\rangle$ corresponds to the ground electronic-first ($v = 1$) vibrational state), thus leading to autocorrelation $\langle i|i(t)\rangle$ and correlation $\langle f|i(t)\rangle$ functions. The Fourier transformation of $\langle i|i(t)\rangle$ multiplied by the damping factor, $\exp(-\Gamma t/\hbar)$ (where Γ contributes to homogeneous broadening) gives the absorption spectrum. Similarly, the square of the half Fourier transformation of $\langle f|i(t)\rangle$ multiplied by the same damping factor gives the Raman excitation profile (REP). In the case of Raman intensity analysis, traditionally, the semiclassical approach using Manneback's recursion formula (Manneback 1951) is used for large polyatomic molecules (Myers and Mathies 1984; Myers *et al* 1982, 1983). However, for small molecules with a few atoms, a rather simple and computationally tractable time-dependent quantum mechanical (TDQM) approach has been proposed by Imre and coworkers (Williams and Imre 1988a) to analyse resonance Raman excitation profiles. This TDQM approach has been successfully used to understand absorption and emission spectra of O_2 (Williams and Imre 1988b) and photodissociation (Kalyanaraman and Sathyamurthy 1993, 1994) processes of systems such as OH and HI.

In this paper, we have applied the TDQM approach to polyatomic systems, since it provides a simple theoretical basis to understand resonance Raman intensities of polyatomics. With this approach, we have successfully generated the absorption spectrum and the REPs for various Raman active modes of modal system, viz. *cis*-stilbene, in order to test the utility of this approach. This has been previously studied semiclassically by Myers and Mathies (1984), and is an interesting system as it undergoes isomerization along a barrierless excited state potential surface within a few femtoseconds. A comparison of our TDQM simulation results with those obtained by the semiclassical method (Myers and Mathies 1984) shows that the TDQM approach is equally viable for polyatomic systems.

We begin with § 2, which discusses resonance Raman intensity analysis from two theoretical viewpoints, a sum-over-states method (time-independent approach) and a time-independent method. In addition, we give a brief outline of the commonly used semiclassical time-dependent (SCTD) technique and the TDQM method. In § 3, we present the computational details of the latter, using *cis*-stilbene as an example. In the final section 4, we report some preliminary results obtained using the TDQM technique on the isomerization dynamics of *trans*azobenzene. The salient features of the TDQM approach are then summarized.

2. Theory

Resonance Raman intensity analysis

Resonance Raman intensities (Albrecht 1961; Tang and Albrecht 1970) can be calculated using either the sum-over-states or the time-dependent method. In the sum-over-states method, the resonance Raman amplitude for the transition from the initial state $|i\rangle$ to the final state $|f\rangle$ (where both the vibrational eigenstates $|i\rangle$ and $|f\rangle$ correspond to the electronic ground state) can be given by the Kramers–Heisenberg–Dirac (KHD)

dispersion expression (Kramers and Heisenberg 1925; Dirac 1927)

$$\alpha_{i\to f}(E_L) = M^2 \sum_v \frac{\langle f|v\rangle\langle v|i\rangle}{E_v - E_i + E_{00} - E_L - i\Gamma}, \tag{1}$$

where E_{00} is the energy separation between the zeroth vibrational levels of the ground and the excited electronic states, E_v the energy corresponding to the vibrational state $|v\rangle$ of the excited electronic state, E_i the zero-point energy of the ground electronic state, E_L the energy of the incident photon, M the electronic transition moment, and Γ the homogeneous broadening.

The complete expression for resonance Raman cross section can be given as,

$$\sigma_{i\to f}(E_L) = 5{\cdot}87 \times 10^{-19} M^4 E_S^3 E_L \left| \sum_v \frac{\langle f|v\rangle\langle v|i\rangle}{E_v - E_i + E_{00} - E_L - i\Gamma} \right|^2, \tag{2}$$

where, E_S is the energy of the scattered photon. Here $E_L, E_S, E_{00}, E_i, E_v$ and Γ are in cm^{-1}, M is in Å, and $\sigma_{i\to f}$ in $Å^2$/molecule.

Evaluation of the resonance Raman cross-section using the sum-over-states approach involves summing over all the vibrational levels of the resonant electronic state. This method, therefore, requires knowledge of all the eigenstates in the excited state surface, which is perhaps intractable for polyatomic molecules. The alternative time-dependent theory of Raman scattering (Lee and Heller 1979; Heller *et al* 1982; Tannor and Heller 1982) has an advantage in that knowledge of all the eigenstates in the excited surface is not required. Further, Heller's approach provides a more transparent physical picture of the dynamics. In the time-dependent picture, the energy denominator in (2) is replaced by an exponential function and the resonance Raman cross section (Lee and Heller 1979) is expressed as a half Fourier transform of the correlation function $\langle f|i(t)\rangle$,

$$\sigma_{i\to f}(E_L) = \frac{8\pi e^4 M^4 E_S^3 E_L}{9\hbar^6 c^4} \left| \int_o^\infty \langle f|i(t)\rangle \exp[i(E_L + E_i)t/\hbar - \Gamma t/\hbar]\,dt \right|^2, \tag{3}$$

where, e is the charge of the electron, c the velocity of light, $\hbar = h/2\pi$ (h being Planck's constant), and $|i(t)\rangle$ is the evolving wavepacket at various intervals of time, under the influence of the excited state Hamiltonian H_{ex}, i.e

$$|i(t)\rangle = \exp(-iH_{ex}t/\hbar)|i\rangle. \tag{4}$$

Similarly, the expression for the absorption cross-section (Kulander and Heller 1978; Heller *et al* 1982) in the time-dependent formalism is

$$\sigma_A(E_L) = \frac{4\pi e^2 M^2 E_L}{6\hbar^2 cn} \int_{-\infty}^{+\infty} \langle i|i(t)\rangle \exp[i(E_L + E_i)t/\hbar - \Gamma|t|/\hbar]\,dt, \tag{5}$$

where, n is the refractive index of the solution.

In (3) and (5) above, the dynamical information is contained in the correlation functions. Therefore, by computing the Raman amplitude and the absorption cross section, and then comparing these data with experimental results, one can learn about the structural dynamics in the excited electronic state.

2.2 *Correlation function calculations*

As described in the introduction, the correlation function calculation requires the

knowledge of $|i(t)\rangle$ in the excited state surface at different times. This is normally obtained by evolving the ground state wave function $|i\rangle$ (at $t = 0$) under the influence of the excited state Hamiltonian (H_{ex}). Two methods, namely, the SCTD and the TDQM, are used to study the evolution of the wavepacket on the excited state surface. Both approaches are compared below. We have considered harmonic as well as linear dissociative excited state potentials. However, it is assumed that the ground and the excited state normal coordinates are identical [with no Duschinsky effect (Siebrand and Zgierski 1979)] and that there are no changes in frequency on going from the ground to the excited state. In the absence of Duschinsky effect, the multidimensional autocorrelation function $\langle i|i(t)\rangle$ will be the product of $\langle i_j|i_j(t)\rangle$, where $j = 1, 2 \ldots . N$ (N being the total number of vibrational modes present in the molecule). Similarly, the multidimensional correlation function $\langle f|i(t)\rangle$ is the product of $\langle f_k|i_k(t)\rangle$ in the Raman active mode (k) and $\langle i_j|i_j(t)\rangle, j = 1, 2 \ldots . (N\text{-}1)$. That is,

$$\langle i|i(t)\rangle = \prod_{j=1}^{N} \langle i_j|i_j(t)\rangle, \tag{6}$$

$$\langle f|i(t)\rangle = \langle f_k|i_k(t)\rangle \prod_{j=1, j\neq k}^{N-1} \langle i_j|i_j(t)\rangle. \tag{7}$$

Both the SCTD and TDQM methods have some common limitations (Myers 1990) viz., (a) accurate ground electronic state normal mode analysis is necessary to interpret Raman intensities in terms of their mode-specific dynamics, (b) nuclear dynamics, occurring only on time scales shorter than the electronic dephasing time, can be studied, and (c) collisionally activated processes are not reflected in the resonance Raman intensitites.

2.3 *Semiclassical time dependent (SCTD) method*

The implementation of the time-dependent formulation of Raman scattering (Heller 1975, 1978, 1981; Lee and Heller 1979; Heller *et al* 1982; Tannor and Heller 1982) makes use of approximate semiclassical methods for the solution of the time-dependent motion of the wave packet. This method gives simple expressions for fundamental and overtone Raman intensities, which depend only on potential energy surface features in the Franck–Condon region. Further, it is assumed that the classical trajectories govern the dynamics of the wavepacket. Assuming the ground and the excited state potentials to be harmonic (so that they can be expressed in dimensionless coordinates (q) as, $V(q) = (1/2)\hbar\omega(q - q_e)^2$, where q_e is the equilibrium value corresponding to the minimum of the potential) and their frequencies (ω) to be identical, the position and the momentum of the centre of the wavepacket is governed by classical dynamics. Thus, the one-dimensional absorption and Raman correlation functions are given by the following forms (Myers *et al* 1982; Tannor and Heller 1982),

$$\langle i|i(t)\rangle = \exp\left[-s(1 - e^{-i\omega t}) - \frac{i\omega t}{2} - \frac{iE_{00}t}{\hbar}\right], \tag{8}$$

$$\langle f|i(t)\rangle = \pm s^{1/2}(e^{-i\omega t} - 1)\langle i|i(t)\rangle, \tag{9}$$

where, $s = \Delta^2/2$ (Δ is the dimensionless displacement). The sign in (9) depends on the sign of Δ. Substituting for the one-dimensional overlaps in (3) and (5), the multidimensional expressions for the fundamental Raman and the absorption cross-sections

(Myers and Mathies 1987) are given as

$$\sigma_{0\to 1}(E_L) = \frac{8\pi E_S^3 E_L e^4 M^4}{9\hbar^6 c^4} \times \left| \int_0^\infty \exp\left[\frac{i(E_L - E_{00})t}{\hbar} - \frac{\Gamma t}{\hbar}\right] s_1^{1/2}(e^{-i\omega_1 t} - 1) \times \prod_{j=1}^{N} \exp(-s_j[1 - \exp(-i\omega_j t)])dt \right|^2, \tag{10}$$

$$\sigma_A(E_L) = \frac{4\pi e^2 M^2 E_L}{6\hbar^2 cn} \times \int_{-\infty}^{+\infty} \exp\left[\frac{i(E_L - E_{00})t}{\hbar} - \frac{\Gamma|t|}{\hbar}\right] \times \prod_{j=1}^{N} \exp(-s_j[1 - \exp(-i\omega_j t)])dt, \tag{11}$$

where mode 1 corresponds to the Raman active mode. From the above expressions it can be observed that in a molecule the Raman amplitudes of various modes differ only by the factors $s_1^{1/2}$ and $(e^{-i\omega_1 t} - 1)$, which are responsible for changes in magnitude and band shape of the REP respectively.

In case of a linear dissociative excited state potential [$V(q) = -\beta q$], where β is the slope of the excited state potential, the one dimensional time-dependent correlation functions (Myers *et al* 1983) are given as

$$\langle i|i(t)\rangle = \left(1 + \frac{i\omega t}{2}\right)^{-1/2} \exp\left[-\frac{\beta^2(6t^2 + i\omega t^3)}{24\hbar^2}\right], \tag{12}$$

$$\langle f|i(t)\rangle = -i2^{-1/2}\left(\frac{\beta t}{\hbar}\right)\langle i|i(t)\rangle. \tag{13}$$

Thus, substituting these values of $\langle f|i(t)\rangle$ and $\langle i|i(t)\rangle$ in (3) and (5), and multiplying by $\exp(-iE_{00}t/\hbar)$, where E_{00} is the energy separation between the ground and the excited state potential, REP and the absorption spectrum can be obtained.

2.4 *Time-dependent quantum mechanical (TDQM) approach*

Unlike the SCTD approach, in this method the initial wave function for the ground electronic–ground vibrational state ($|i\rangle$) for a harmonic oscillator is first computed and then transposed to the excited electronic state after multiplying with the transition dipole moment. The propagation of the transposed wave function in the excited electronic state is obtained by solving the time-dependent Schrödinger equation, using standard methodology (Feit *et al* 1982; Kosloff and Kosloff 1983a, b; Kosloff 1988; Mohan and Sathyamurthy 1988). Once the propagated wavepacket $|i(t)\rangle$ is obtained, the autocorrelation function, $\langle i|i(t)\rangle$ and the correlation function, $\langle f|i(t)\rangle$ can be computed.

In this method, the main objective is to solve the time-dependent Schrödinger equation,

$$i\hbar\frac{\partial\psi_v(q,t)}{\partial t} = H_{ex}\psi_v(q,t), \tag{14}$$

where

$$H_{ex} = -(1/2)\hbar\omega\frac{\partial^2}{\partial q^2} + V(q), \tag{15}$$

and, $\psi_v(q, t=0)$ is the wave function corresponding to a particular vibrational state (v) in the ground electronic state. For a harmonic oscillator

$$\psi_v(q) = N_v H_v(q)\exp[(-1/2)(q-q_e)^2], \tag{16}$$

where N_v is the normalization constant and H_v the Hermite polynomial corresponding to the vth vibrational state.

The wave function $\psi_v(q)$ is computed in a spatial grid which satisfies the following conditions: (i) the grid must be large enough to accommodate the wave functions of all states, and the magnitude of the wave functions should be negligible at the boundary, and (ii) the grid spacings should be small enough to resolve the ground state wave function and to accommodate the spatial bandwidth of the wave function. In the present study, the initial wavefunction $\psi_0(q, t=0)$ or $|i\rangle$ is specified on a chosen grid of 2048 points with a grid spacing of 0·1 dimensionless units. The time evolution of the wavefunction on the excited state is given by

$$|i(t)\rangle = \hat{U}|i(t_0)\rangle, \tag{17}$$

where t_0 corresponds to zero time and $\hat{U}$ is the time evolution operator:

$$\hat{U} = \exp(-iH_{ex}\Delta t/\hbar), \quad \Delta t = t - t_0. \tag{18}$$

In practice, the propagator is sliced at several time intervals and at each time step, a fourth-order finite difference (Manthe and Köppel 1990a, b) scheme is used to represent $\hat{U}$. In the present calculation, the time evolution involves a total of 8192 steps with each step (Δt) corresponding to 0·01 fs.

The integrals $\langle i|i(t)\rangle$ and $\langle f|i(t)\rangle$ are computed using the extended Simpson's rule (Abramowitz and Stegun 1968). Similar to the SCTD case, the absorption and resonance Raman cross sections can be computed by substituting $\langle i|i(t)\rangle$ and $\langle f|i(t)\rangle$ in (3) and (5).

3. Simulation for *cis*-stilbene

The experimentally observed vibrational modes of *cis*-stilbene (Warshel 1975; Myers and Mathies 1984), their respective frequencies and the relative dimensionless displacements (Δ) are given in table 1 and the exact values for M, E_{00}, β and Δ, have been taken from Myers and Mathies (1984, 1987). The TDQM method has been applied to generate the absorption spectrum and the REPs. The values of M, E_{00}, β and Δ are the variables normally used in the simulation, to match the Raman amplitudes and absorption spectrum with the experimental data. In the following part, we give one example each of a single mode calculation for a linear dissociative and a harmonic excited state potential. Many other vibrational mode calculations are not shown since they follow similar behaviour except for changes in amplitude and shape of the $\langle i|i(t)\rangle$ and $\langle f|i(t)\rangle$.

3.1 *Single mode correlation functions*

Firstly, a single mode that is dissociative with vibrational frequency $\omega = 560\,\text{cm}^{-1}$,

Table 1. Frequencies and excited state displacements of various vibrational modes of *cis*-stilbene (Warshel 1975; Myers and Mathies 1984).

Description of vibrational modes[1]	Frequency (in cm^{-1})	Dimensionless displacement $\|\Delta\|$
ϕ–C=C ben	165	4·4
oop ring def	403	1·73
H oop wag	963	1·16
Trigonal ring def	1001	0·67
ring H rocik, C–ϕ str	1187	0·70
C–C–H ben	1233	0·40
Ring str, vinyl H rock	1328	0·52
Ring str	1490	0·38
Ring str	1575	0·64
Ring str	1600	1·05
Ethylenic C=C str	1629	1·60

[1]Description of vibrations:
tor:torsion, def: deformation, oop:out of plane, ben bending, str:stretching.

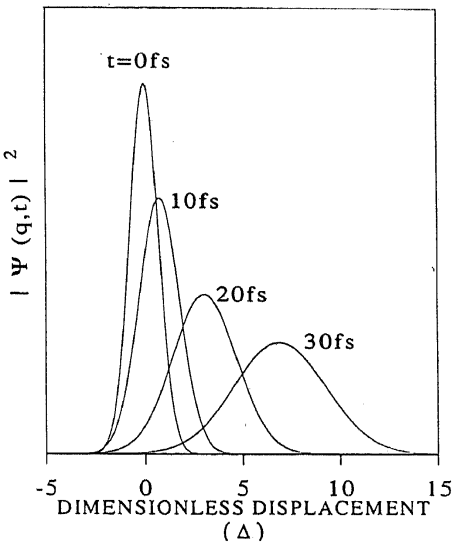

Figure 1. Moving wavepacket picture for dynamics on a linear dissociative excited state potential surface.

$E_{00} = 29300\,cm^{-1}$ and $M = 0{\cdot}9$ Å is considered. This mode (j) corresponds to torsion about the central C–C double bond of *cis*-stilbene. In this case, the autocorrelation function, $\langle i_j | i_j(t) \rangle$ will be maximum at time $t = 0$ and it decays eventually to zero as the wavepacket $|i_j(t)\rangle$ moves away from the Franck–Condon region. The moving wavepacket on a linear dissociative potential at different times (t) is shown in figure 1. The calculated autocorrelation, $|\langle i_j | i_j(t) \rangle|$, (solid line) and the Raman correlation functions, $|\langle f_j | i_j(t) \rangle|$, (dotted line) for $\omega = 560\,cm^{-1}$ are shown in figure 2. The Raman correlation function is zero at the start but it increases to a maximum as $|i_j(t)\rangle$ overlaps maximum with $|f_j\rangle$ and decreases as it moves further away.

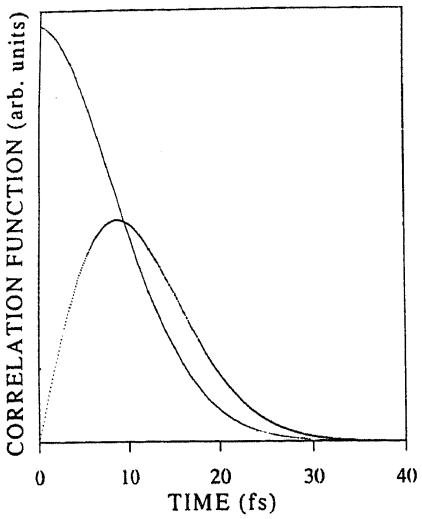

Figure 2. Autocorrelation, $|\langle i_j|i_j(t)\rangle|$ (solid line) and Raman correlation function, $|\langle f_j|i_j(t)\rangle|$ (dotted line), where j corresponds to C_e–C_e torsional mode (linear dissociative) with frequency $\omega = 560\,\text{cm}^{-1}$.

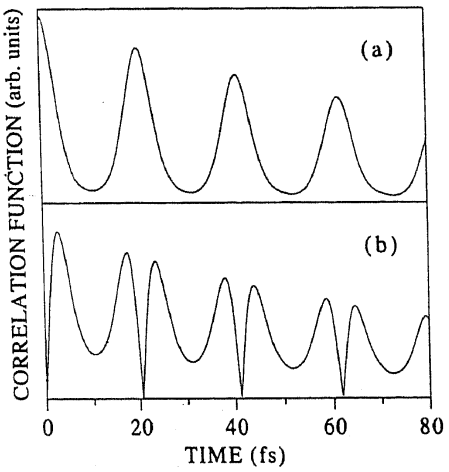

Figure 3. (**a**) Autocorrelation function, $|\langle i_j|i_j(t)\rangle|$, and (**b**) Raman correlation function, $|\langle f_j|i_j(t)\rangle|$, where j corresponds to C_e–C_e torsional mode (harmonic) with frequency $\omega = 1629\,\text{cm}^{-1}$.

In the case of ethylenic C–C stretching mode with frequency ω ($1629\,\text{cm}^{-1}$), the excited state potential is assumed to be harmonic and the autocorrelation and Raman correlation functions are expected to consist of periodic recurrences. This is due to the fact that the wavepacket moves back and forth, thus appearing again in the Franck–Condon region, after a vibrational period. The autocorrelation function, $|\langle i_j|i_j(t)\rangle|$ and the Raman correlation function, $|\langle f_j|i_j(t)\rangle|$ for $\omega = 1629\,\text{cm}^{-1}$ and $\Gamma = 50\,\text{cm}^{-1}$ are shown in figures 3(a) and 3(b) respectively.

3.2 *Multimode correlation functions*:

The multimode autocorrelation function $\langle i|i(t)\rangle$ is computed by taking the product of all the $\langle i_j|i_j(t)\rangle$ for the various vibrational modes (j). Similarly, the Raman correlation function $\langle f|i(t)\rangle$ is computed by taking the product of $\langle f_k|i_k(t)\rangle$ for the Raman active

mode (k) and $\langle i_j|i_j(t)\rangle$ for the rest of the modes (j). At $t = 0$, all the modes are in phase and hence $|\langle i|i(t)\rangle|$ is maximum, but as time increases these modes get out of phase. As a result, the multimode autocorrelation function decays within 10 fs as shown in figure 4a and it does not show any recurrence up to 100 fs. The multimode Raman correlation function first increases from zero to a maximum value and then decays irreversibly as expected. $|\langle f|i(t)\rangle|$ for 560 and 1629 cm^{-1} and 1629 cm^{-1} are shown in figures 4(b) and (c) respectively. The simulated absorption spectrum obtained by full Fourier transformation of the multimode autocorrelation function is shown in figure 5(a) and the REPs for 560 and 1629 cm^{-1} modes, obtained by half Fourier transformation of the respective multimode Raman correlation functions, are shown in figures 5(b) and (c) respectively.

A comparison of the figures available for various autocorrelation and Raman correlation functions, from Myers and Mathies (1984, 1987), Myers (1990) and from our

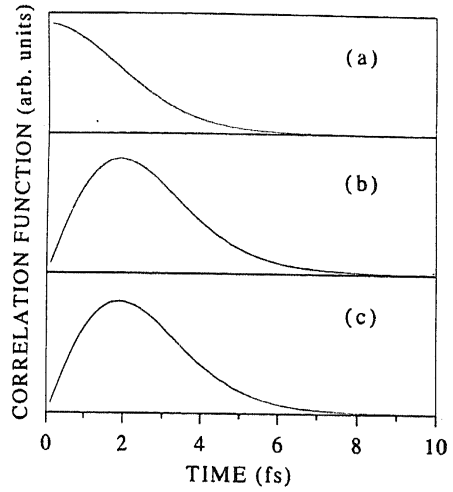

Figure 4. (a) Multimode autocorrelation function, $|\langle i|i(t)\rangle|$; (b) Multimode Raman correlation function, $|\langle f|i(t)\rangle|$ for C_e–C_e torsion ($\omega = 560\,cm^{-1}$), and (c) for C_e–C_e stretch ($\omega = 1629\,cm^{-1}$).

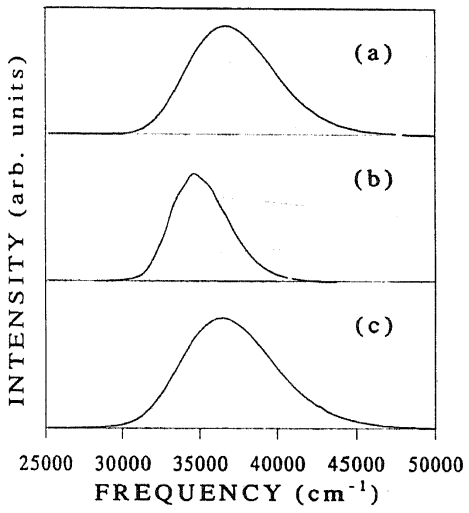

Figure 5. (a) Simulated absorption spectrum; (b) Simulated REPs of *cis*-stilbene for C_e–C_e torsion ($\omega = 560\,cm^{-1}$), and (c) C_e–C_e stretch ($\omega = 1629\,cm^{-1}$).

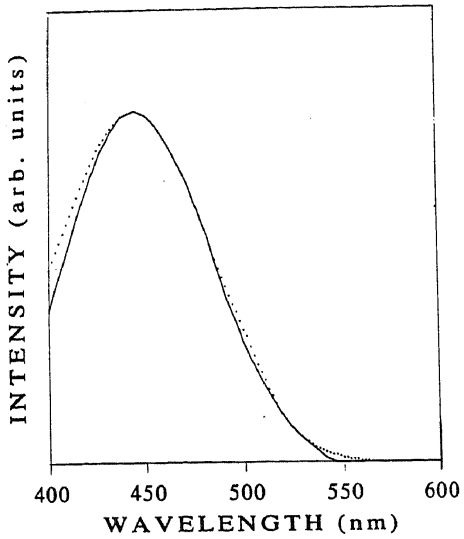

Figure 6. Simulated (dotted line) and experimental (solid line) absorption spectrum of *trans*-azobenzene.

calculation reveals that they are very similar thus demonstrating the practicability of the TDQM method for polyatomic systems.

4. Azobenzene as a new model system

In order to study the dynamics (including the mechanism) of isomerization, the time-dependent wavepacket propagation technique has been applied to *trans*- azobenzene. It undergoes isomerization upon UV [$^1(\pi - \pi^*)$] or VIS [$^1(n - \pi^*)$] excitation. The quantum yield ($\phi_{trans \to cis}$) of isomerization depends on both wavelength and temperature (Rau 1990). $\phi_{trans \to cis}$) has been found to be greater for $^1(n - \pi^*)$ excitation than for $^1(\pi - \pi^*)$. There has also been a debate in the literature about the nature of the state (singlet or triplet) participating in the isomerization of *trans*-azobenzene, and also the possible routes of isomerization, *viz.*, rotation or inversion (Rau 1990).

In *trans*-azobenzene, we have selected the 912 cm^{-1} mode to be dissociative along which possibly inversion (or ϕ–N=N–ϕ torsion) occurs, as has been proposed by Lorriaux *et al* (1979). In order to get the best fit absorption spectrum, the simulated values of zero-zero energy (E_{00}), homogeneous broadening (Γ), transition dipole moment (M) and the slope of linear dissociative potential are 20470 cm^{-1}, 50 cm^{-1}, 0·8 Å and 980 cm^{-1} in that order. The simulated absorption spectrum (dotted line) obtained by the TDQM method compares very small well with the experimental one (solid line) as shown in figure 6. Further work is in progress along the direction of simulating the experimental Raman excitation profiles reported earlier (Okamoto *et al* 1986) for the Raman active modes of *trans*-azobenzene and thereby, propose a suitable mechanism for isomerization (Biswas and Umapathy 1995).

Summary

We have demonstrated that the implementation of the TDQM method is straightforward and that one can compute the absorption spectrum and the Raman excitation

profile which are comparable to the experimental results. Using the TDQM approach, we could obtain information on the displacements at anytime after excitation but before the electronic dephasing time, since the computation involves a stepwise approach.

The relative dimensionless displacements derived from the moving wavepacket picture or the excitation profile simulation for different vibrational modes, can be related to the internal coordinates (i.e bond length, bond angle and dihedral angle) of a given system. Changes in the internal coordinates for the respective vibrational mode at different times, thus lead us to visualize the nuclear motion in the primary stages of a photoexcited process. For systems which undergo structural changes on excitation in the early femtosecond time scale and which cannot be studied experimentally, this (theoretical) time dependent approach is the best alternative. Further work is in progress in using this TDQM technique for systems like azobenzene which undergo ultrafast isomerization dynamics.

Acknowledgements

We thank Professors J Chandrasekhar and B J Cherayil for helpful discussions and acknowledge the financial assistance from the Council of Scientific and Industrial Research, New Delhi and the Department of Science and Technology, New Delhi.

List of symbols

$\|i\rangle$	ground electronic and vibrational state ($v = 0$);
$\|f\rangle$	ground electronic first vibrational state ($v = 1$);
$\|i(t)\rangle$	moving wavepacket on the excited state surface;
Γ	homogeneous broadening;
$\langle i\|i(t)\rangle$	autocorrelation function;
$\langle f\|i(t)\rangle$	correlation function;
$\|v\rangle$	vibrational states of the excited electronic state;
$\sigma_{i\to f}$	Raman cross section;
σ_A	absorption cross section;
Δt	relative changes in time;
Δ	relative dimensionless displacement;
ω	vibrational frequency;
β	slope of the linear dissociative potential;
$\psi_v(q,t)$	vibrational state (v) as a function of dimensionless coordinate (q) and time (t);
$\partial/\partial t$	derivative with respect to time;
$\partial^2/\partial q^2$	Laplacian operator;
$\hat{U}$	forward time evolution operator;
$^1(\pi-\pi^*)$, $^1(n-\pi^*)$	electronic states;
$\phi_{trans\to cis}$	quantum yield for *trans* to *cis* isomerization;
ϕ	phenyl ring.

References

Abramowitz M and Stegun I A 1968 *Handbook of mathematical functions* (New York: Dover) p. 886

Albrecht A C 1961 *J. Chem. Phys.* **34** 1476

Biswas N and Umapathy S 1995 *Chem. Phys. Lett.* **236** 24
Dirac P A M 1927 *Proc. R. Soc. (London)* **114** 710
Feit M D, Fleck J A Jr, and Steiger A 1982 *J. Comput. Phys.* **47** 412
Heller E J 1975 *J. Chem. Phys.* **62** 1544
Heller E J 1978 *J. Chem. Phys.* **68** 2066
Heller E J 1981 *Acc. Chem. Res.* **14** 368
Heller E J, Sundberg R L and Tannor D J 1982 *J. Phys. Chem.* **86** 1822
Kalyanaraman C and Sathyamurthy N 1993 *Chem. Phys. Lett.* **209** 52
Kalyanaraman C and Sathyamurthy N 1994 *Chem Phys.* **187** 219
Kosloff D and Kosloff R 1983a *J. Comput. Phys.* **52** 35
Kosloff R and Kosloff D 1983b *J. Chem. Phys.* **79** 1823
Kosloff R 1988 *J. Phys. Chem.* **92** 2087
Kramers H A and Heisenberg W 1925 *Z. Phys.* **31** 681
Kulander K C and Heller E J 1978 *J. Chem. Phys.* **69** 2439
Lee S Y and Heller E J 1979 *J. Chem. Phys.* **71** 4777
Lorriaux J L, Merlin J C, Dupaix A and Thomas E W 1979 *J. Raman Spectrosc.* **8** 81
Manneback C 1951 *Physica* **17** 1001
Manthe U and Köppel H 1990a *J. Chem. Phys.* **93** 345
Manthe U and Köppel H 1990b *J. Chem. Phys.* **93** 1658
Mohan V and Sathyamurthy N 1988 *Comput. Phys. Rep.* **7** 215
Myers A B 1990 *J. Opt. Soc. Am. B*, **7** 1665
Myers A B and Mathies R A 1984 *J. Chem. Phys.* **81** 1552
Myers A B and Mathies R A 1987 *Biological applications of Raman spectroscopy* (ed.) T G Spiro (New York: John Wiley and Sons) vol 2, p. 1
Myers A B, Mathies R A, Tannor D J and Heller E J 1982 *J. Chem. Phys.* **77** 3857
Myers A B, Harris R A and Mathies R A 1983 *J. Chem. Phys.* **79** 603
Okamoto H, Hamaguchi H and Tasumi M 1986 *Chem. Phys. Lett.* **130** 185
Ramakrishna M V and Coalson R D 1988 *Chem. Phys.* **120** 327
Rau H 1984 *J. Photochem.* **26** 221
Rau H 1990 *Photochromism: molecules and systems* (eds) H Durr and H Bouas-Lauren (Amsterdam: Elsevier.) chap. 4, p. 165
Siebrand W and Zgierski M Z 1979 *Chem. Phys. Lett.* **62** 3
Tang J and Albrecht A C 1970 *Raman Spectroscopy* (ed) H A Szymanski (Plenum: New York) vol. 2, p. 33
Tannor D J and Heller E J 1982 *J. Chem. Phys.* **77** 202
Warshel A 1975 *J. Chem. Phys.* **62** 214
Williams S O and Imre D G 1988a *J. Phys. Chem.* **92** 3363
Williams S O and Imre D G 1988b *J. Phys. Chem.* **92** 3374